Carbohydrate Polymers 75 (2009) 705–711

Contents lists available at ScienceDirect

Carbohydrate Polymers

journal homepage: www.elsevier.com/locate/carbpol

# Structural characterization of wheat starch granules differing in amylose content and functional characteristics

Jaroslav Blazek [a], Hayfa Salman [a], Amparo Lopez Rubio [b], Elliot Gilbert [b], Tracey Hanley [b], Les Copeland [a,*]

[a] Faculty of Agriculture, Food and Natural Resources, University of Sydney, NSW 2006, Australia
[b] Bragg Institute, Australian Nuclear Science and Technology Organisation, Private Mail Bag 1, Menai, NSW 2234, Australia

ARTICLE INFO

*Article history:*
Received 4 February 2008
Received in revised form 27 August 2008
Accepted 12 September 2008
Available online 23 September 2008

*Keywords:*
Wheat starch
*Triticum aestivum*
Amylose
Amylopectin
Small-angle X-ray scattering
Granule structure
X-ray diffraction
Differential scanning calorimetry

ABSTRACT

Small-angle X-ray scattering (SAXS) together with several complementary techniques, such as differential scanning calorimetry and X-ray diffraction, have been employed to investigate the structural features that give diverse functional properties to wheat starches (*Triticum aestivum* L.) within a narrow range of enriched amylose content (36–43%). For these starches, which come from a heterogeneous genetic background, SAXS analysis of duplicate samples enabled structural information to be obtained about their lamellar architecture where differences in lamellar spacing among samples were only several tenths of nanometer. The SAXS analysis of these wheat starches with increased amylose content has shown that amylose accumulates in both crystalline and amorphous parts of the lamella. Using waxy starch as a distinctive comparison with the other samples confirmed a general trend of increasing amylose content being linked with the accumulation of defects within crystalline lamellae. We conclude that amylose content directly influences the architecture of semi-crystalline lamellae, whereas thermodynamic and functional properties are brought about by the interplay of amylose content and amylopectin architecture.



## 1. Introduction

Semi-crystalline native starch granules display a hierarchical structural periodicity. Starch granules have a layered organization with alternating amorphous and semi-crystalline radial growth rings of 120–400 nm thickness emanating from the hilum. The amorphous rings consist of amylose and amylopectin in a disordered conformation, whereas the semi-crystalline rings are formed by a lamellar structure of alternating crystalline and amorphous regions with a repeat distance of 9–11 nm (Cameron & Donald, 1992). The crystalline regions of the lamellae are mainly formed by double helices of amylopectin side chains packed laterally into a crystalline lattice, whereas amorphous regions contain amylose and the amylopectin branching points. Amylopectin clusters may contain amylose molecules that pass through both the crystalline and amorphous layers. These "tie-chain" amylose molecules are proposed to be in a straightened conformation in crystalline regions and in a disordered conformation in amorphous regions (Kozlov, Blennow, Krivandin, & Yuryev, 2007a; Matveev et al., 1998).

Small-angle X-ray scattering (SAXS) techniques measure differences in electron density distribution, whereas diffraction techniques are indicative of crystallinity of the material. SAXS and neutron scattering have been shown to be useful for studying the arrangement of lamellar structures in semi-crystalline starch granules (Waigh, Jenkins, & Donald, 1996). SAXS patterns from hydrated native starches show a broad scattering peak, from which the average thickness of the lamellar repeat unit (that is the thickness of the crystalline plus amorphous layers) can be calculated. In combination with other techniques, such as differential scanning calorimetry (DSC) and X-ray diffraction (XRD), the thickness of the crystalline layer can be calculated (Blanshard, Bates, Muhr, Worcester, & Higgins, 1984; Waigh, Gidley, Komanshek, & Donald, 2000a; Waigh, Kato, Donald, Gidley, & Riekel, 2000b; Waigh, Perry, Riekel, Gidley, & Donald, 1998). The position of the SAXS peak is related to the average lamellar repeat length in granular starches, whereas peak width and intensity are mainly dependent on the regularity of the arrangement of lamellae and the electron density differences between the amorphous and crystalline regions of the lamellar structure. Recent studies using SAXS and high-sensitivity DSC have increased our understanding of the influence of amylose located within amylopectin clusters in native starch granules (Kozlov, Noda, Bertoft, & Yuryev, 2006). SAXS has also proved useful in helping to describe processes such as swelling, gelatinization, retrogradation and annealing (Donald, Kato, Perry, & Waigh, 2001; Lopez-Rubio, Htoon, & Gilbert, 2007; Vermeylen, Goderis, Reynaers, & Delcour, 2005; Vermeylen et al., 2006).

Several approaches aimed at obtaining wheat starches with increased amylose content have been reported in the literature.

* Corresponding author. Tel.: +61 2 9036 7047; fax: +61 2 9351 2945.
*E-mail address:* l.copeland@usyd.edu.au (L. Copeland).

0144-8617/$ - see front matter © 2008 Elsevier Ltd. All rights reserved.
doi:10.1016/j.carbpol.2008.09.017

Some of the breeding programs are based on the genetic manipulation of the enzymes involved in starch synthesis (Kozlov et al., 2006; Morell & Myers, 2005), whereas selecting among wheat varieties with increased amylose content for functional characteristics has also been reported to lead towards the increase in amylose content (Blazek & Copeland, 2008). Different breeding approaches can result in starches with increased amylose that vary in their functional, structural and thermodynamic characteristics. For example, wheat varieties with increased amylose content described by Hung, Maeda, and Morita (2007) had levels of crystallinity comparable to starches with normal amylose content, whereas another study using a different breeding strategy found increased amylose content to be accompanied with a loss of crystallinity (Hung, Maeda, Miskelly, Tsumori, & Morita, 2008).

The varieties used in this study, and those described by Blazek and Copeland (2008) and Hung et al. (2008), were obtained by genetic back-crossing of wheat cultivars grown in Australia. The swelling power test was used as a simple screening method to select lines for increased amylose content; hence, the genetic background of these wheat cultivars was not uniform. These starches have been shown to have a gradation of pasting, swelling and thermodynamic characteristics correlated to amylose content (Blazek & Copeland, 2008; Hung et al., 2008). In this study, SAXS together with DSC, XRD and fluorophore-assisted capillary electrophoresis, were employed to further examine structural features that provide these starches with a wide range of functional properties within a narrow range of enriched amylose content.

## 2. Materials and methods

### 2.1. Materials

Twelve wheat (*Triticum aestivum* L.) varieties selected from the set of samples described by Blazek and Copeland (2008) were used in the study. These included 10 varieties with increased amylose content produced through the Value Added Wheat CRC Ltd (VAWCRC) breeding program, one waxy variety and starch extracted from commercial flour. This breeding program is based on commercial Australian hard wheat cultivars of diverse genetic background. Samples used in the study were grown in Eastern Australia over three growing seasons. Starch was extracted from flour using a two-step procedure that involved enzymic removal of proteins and subsequent extraction of free lipids with ethanol, based on the method of Akerberg, Liljeberg, Granfeldt, Drews, and Bjorck (1998) as described by Blazek and Copeland (2008).

Total amylose (T-AM) and free amylose (F-AM) content were determined by iodine binding as described by Chrastil (1987) using a calibration curve derived from a set of maize starches with zero to 75% amylose. According to this method, total and free amylose values were obtained from iodine binding with and without lipid extraction by ethanol, respectively. Lipid-complexed amylose (L-AM) was calculated as the difference between T-AM and F-AM. Amylopectin chain length distribution was determined in the laboratories of CSIRO Plant Industry, Canberra, by fluorophore-assisted capillary electrophoresis using the Beckman P/ACE System 5010, as described by Morell, Samuel, and O'Shea (1998) and O'Shea, Samuel, Konik, and Morell (1998).

Starch swelling power (SSP) was determined by measuring water uptake at 92.5 °C by a 40 mg sample of starch according to the method of Konik-Rose et al. (2001) as described by Blazek and Copeland (2008). The swelling power test was carried out in 0.1% $AgNO_3$ solution to inhibit α-amylase activity. Particle size distribution was determined in the laboratories of Allied Mills, Sydney using a Mastersizer laser diffraction instrument in wet-cell mode. Prior to analysis, starch samples were dispersed in deionized water and filtered through a 63 μm sieve. Results are presented as the ratio of particles of diameter less than 10 μm (assumed to be mostly B granules) to particles with diameter between 10 and 35 μm (assumed to be mostly A granules).

### 2.2. Small-angle X-ray scattering

SAXS measurements were obtained with a Bruker Nanostar SAXS camera, with pin-hole collimation for point focus geometry. The X-ray source was a copper rotating anode (0.1 mm filament) operating at 50 kV and 24 mA, fitted with cross coupled Göbel mirrors, resulting in a Cu $K_\alpha$ radiation wavelength of 1.5418 Å. The SAXS camera was fitted with a Hi-star 2D detector (effective pixel size 100 μm). The sample to detector distance was chosen to be 650 mm, which provided a $q$-range from 0.02 to 0.3 $Å^{-1}$, where $q$ is the magnitude of the scattering vector defined as:

$$q = \frac{4\pi}{\lambda}\sin\theta,$$

with $\lambda$ the wavelength and $2\theta$ the scattering angle. Starch samples were presented in 2 mm sealed glass capillaries. Scattering data of starch samples were collected as starch suspensions containing excess water above the settled starch granules. SAXS curves of waxy starch and starch extracted from commercial flour were collected once only, whereas nine replicate SAXS curves of the 10 starch samples from the VAWCRC were collected using separate capillaries; the enhanced precision offered by measuring sufficient replicates allowed subtle differences in lamellar architecture to be discerned. The optics and sample chamber were under vacuum to minimize air scattering. Scattering files were normalized to sample transmission, and after subtracting background, averaged radially using macros written in the Igor software (Wavemetrics, Lake Oswego, Oregon, USA). SAXS curves were plotted as a function of relative peak intensity, $I$, versus $q$, the scattering vector.

The parameters of the SAXS peaks of the varieties with increased amylose content, namely the thickness of the lamella and thicknesses of the crystalline and amorphous regions of the lamella, were determined by considering the ideal lamellar model, which consists of alternating crystalline and amorphous lamellae that are placed in stacks with dimensions that are large enough not to affect the small-angle scattering (Balta Calleja & Vonk, 1989; Koberstein & Stein, 1983; Strobl & Schneider, 1980). The model is assumed to be isotropic, that is it has no preferred orientation. Extrapolated scattering curves were Fourier transformed into a one dimensional correlation function using the CORFUNC program (part of the CCP13 suite of software). The correlation function was interpreted in terms of an ideal lamellar morphology using Igor software and a curve fitting approach to obtain structural parameters describing the sample, namely the long period $L_p$ (also known as Bragg spacing $d$ or lamellar repeat distance), hard block thickness $L_c$ and soft block thickness $L_a$. Electron density contrast was calculated from the one dimensional correlation function. The intensity of the scattering peak was determined by the graphical method as described by Yuryev et al. (2004). Waxy and commercial samples used in this study were analyzed by the same graphical method to determine repeat distance and peak intensity.

An alternative approach is to invoke the model proposed by Daniels and Donald (2003). However, this model utilizes eight adjustable parameters to account for the small-angle scattering. In the absence of additional scattering information, such as that obtained with combined neutron contrast variation methods and subsequent simultaneous global refinement, this method produces significant uncertainties in the fitting parameters, which limits its application. Hence, we used the simpler approach to allow comparison to be made between samples.

### 2.3. X-ray diffraction

XRD measurements of starch samples were made with a Difftech Mini Materials Analyser X-ray diffractometer (GBC Scientific Equipment Pty. Ltd.). The X-ray generator was equipped with a cobalt anode ($\lambda$ = 1.78897 Å) operating at 1 kW and 3.36 mA. X-ray diffractograms were acquired at room temperature (20 ± 1 °C) over the 2$\theta$ range of 5–35° at a rate of 0.50° 2$\theta$ per minute and a step size of 0.05° 2$\theta$. Traces software v. 6.7.13 (GBC Scientific Equipment Pty. Ltd.) was used to manually subtract the background representing the amorphous portion of diffractograms. Starch crystallinity was calculated as a ratio of the crystalline area to the amorphous area. Perfection of the crystalline structures of the samples was assessed based on the full width at half maximum values of selected peaks typical for type A crystallinity.

### 2.4. Differential scanning calorimetry

DSC measurements were made using a Modulated Differential Scanning Calorimeter MDSC 2920 instrument (TA Instruments Inc., Delaware, USA). Starch and deionized water were weighed directly into an aluminum pan at a starch:water ratio of 1:2, and the pan was hermetically sealed. An empty pan was used as a reference. The pans were heated from 30 to 140 °C with the temperature increased at a rate of 10 °C/min. The instrument was calibrated using indium as a standard. Melting temperatures were determined from the thermograms by means of the Universal Analysis 2000 software provided by the instrument company. Calorimetric enthalpy ($\Delta H_m$) was determined by numerical integration of the area under the peak of thermal transition above the extrapolation lines. The average values of the thermodynamic parameters were determined using duplicate measurements and normalized per mole of anhydroglucose units (162 g mol$^{-1}$).

### 2.5. Scanning electron microscopy

Electron micrographs of the starch granules were acquired with a Philips XL30 scanning electron microscope. Samples were mounted on double-sided carbon tape, coated with gold and imaged under an accelerating voltage of 10 kV.

### 2.6. Statistical analysis

All chemical analyses were performed using separate duplicate samples. Correlation analysis was performed using XLStat software (Addinsoft, New York, NY). Pearson's correlation coefficients (r) were calculated between pairs of measured characteristics. A statistically significant relationship between two variables is indicated at the level of statistical significance of $p < 0.05$. The minimum $r$ value for significance at $p = 0.05$ for $n = 10$ samples is 0.632. The starch from the waxy wheat and commercial flour were excluded from the statistical analysis so as not to distort the correlation coefficients by artificially increasing the range of measured characteristics. Moreover, the samples from the VAWCRC program were grown, stored and milled under similar conditions, whereas the waxy line and commercial sample were provided as flours.

## 3. Results

### 3.1. Composition and pasting properties of wheat starches

The composition, swelling properties, melting temperature and chain length distribution of amylopectin of the starches isolated from the cultivars used in this study are summarized in Table 1. Excluding the starches from the waxy wheat and commercial flour, these starches had between 53% and 59% of particles with size distribution between 10 and 35 μm (assumed to be mainly A granules). Total, free and lipid-complexed amylose content varied between 36% and 43%, 28% and 33% and 6% and 14%, respectively. Starch swelling power ranged between 5.4 and 6.9 (Table 1).

Starch extracted from the commercial flour had 35% total amylose, swelling power of 6.3 and contained 57% of particles with size distribution between 10 and 35 μm. The waxy wheat variety included in the study as a comparison, had 4% total amylose content and contained 48% of supposed A granules. Swelling power of the isolated waxy starch was not measurable by the method used in this study.

Scanning electron micrographs of starch granules of the waxy variety and of the amylose-rich varieties (SM1118 is shown as a representative) indicated there were no obvious morphological differences between the granules of the starches examined in this study (Fig. 1). Granules smaller than 10 μm in diameter—assumed to be B granules—displayed round, ellipsoidal, as well as angular and irregular shapes. The surface of most of the granules with diameter greater than 10 μm from all studied wheat varieties displayed indentations, which are likely to be caused by impressions from B granules and protein bodies.

### 3.2. Amylopectin chain length distribution

The amylopectin chains were classified into four fractions according to chain length. These were short chains with degree of polymerization (DP) 6–12, medium length chains with DP 13–24, long chains with DP 25–36, and very long chains with DP greater than 36. The proportions of the fractions in all of the samples were 41–45% of short chains, 46–49% of medium length chains, 7–9% of long chains and less than 2% of very long chains (Table 1). Starches from VAWCRC breeding program had smaller proportions of short chains and greater proportions of long chains as compared to the waxy and commercial starches. No apparent trends or differences were observed among the starches from VAWCRC breeding program (Table 1).

### 3.3. Crystallinity and thermal characteristics

XRD patterns of the selected starches are shown in Fig. 2. All of the starches studied displayed A-type crystallinity with peaks at 17.6°, 19.9°, 20.8° and 26.7° 2$\theta$. Based on the full width at half maximum of the characteristic peaks, waxy wheat displayed the most perfect crystalline structures, whereas the commercial starch showed the least perfect crystallites. The XRD patterns of the 10 varieties from the VAWCRC program were qualitatively very similar and differences in total crystallinity and perfection of the crystal structures could not be quantified due to inherent uncertainties of the method related to the definition of the amorphous background and peak overlay. A peak fitting procedure described by Lopez-Rubio, Flanagan, Gilbert, and Gidley (2008) may allow calculation of starch crystallinity and contribution from the different crystal polymorphs of starch to the total crystallinity, but the quality of the experimental data and differences among traces were not sufficient to use this method.

DSC data showed that the gelatinization temperatures of starches isolated from the varieties from the VAWCRC program varied from 61.5 to 65.4 °C (Table 1). Waxy wheat had higher melting temperature of 66.8 °C, consistent with the increased degree of crystallinity observed by XRD. Starch from the commercial flour had a melting temperature of 62.1 °C. Based on the area under the peak of thermal transition, the transition enthalpy of waxy starch was 1303 kJ/mol, whereas the enthalpies of the commercial starch and variety SM1046 were 996 kJ/mol and 1211 kJ/mol, respectively (Fig. 3).

**Table 1**
Summary of the properties of the starches used in this study

| | T-AM (%) | F-AM (%) | L-AM (%) | SSP (W/W) | A granules (%) | $T_m$ (°C) | DP 6–12 (%) | DP 13–24 (%) | DP 25–36 (%) | DP>36 (%) | $L_p$ (A) | $L_a$ (A) | $L_c$ (A) |
|---|---|---|---|---|---|---|---|---|---|---|---|---|---|
| Waxy starch | 4.1 | – | – | – | 48.1 | 66.8 | 43.6 | 46.9 | 7.9 | 1.6 | – | – | – |
| Commercial starch | 35.2 | 29.5 | 5.7 | 6.3 | 57.3 | 62.1 | 45.0 | 46.2 | 7.4 | 1.4 | – | – | – |
| Diamond bird | 36.1 | 29.9 | 6.2 | 6.3 | 58.2 | 61.5 | 43.0 | 47.0 | 8.4 | 1.6 | 93.38 | 23.53 | 69.84 |
| Ega Hume | 36.8 | 30.7 | 6.2 | 6.9 | 58.0 | 65.0 | 41.9 | 47.7 | 8.7 | 1.8 | 92.91 | 23.54 | 69.37 |
| Batavia | 37.1 | 29.8 | 7.2 | 6.5 | 55.9 | 63.8 | 41.5 | 48.4 | 8.3 | 1.8 | 91.82 | 23.37 | 68.44 |
| Pelsart | 37.8 | 31.9 | 5.9 | 6.0 | 53.2 | 64.0 | 42.0 | 48.0 | 8.4 | 1.7 | 92.64 | 23.39 | 69.25 |
| SM1118 | 38.8 | 33.2 | 5.6 | 5.4 | 57.1 | 64.5 | 41.7 | 48.6 | 8.1 | 1.6 | 92.94 | 23.59 | 69.35 |
| Minto | 39.2 | 30.1 | 9.1 | 6.4 | 55.5 | 65.4 | 41.5 | 48.4 | 8.4 | 1.7 | 92.53 | 23.52 | 69.01 |
| OA24-328-1 | 40.2 | 31.0 | 9.2 | 6.0 | 57.5 | 64.0 | 42.3 | 47.7 | 8.4 | 1.6 | 94.31 | 23.85 | 70.46 |
| OA24-328-3 | 41.2 | 33.1 | 8.1 | 5.8 | 59.2 | 64.1 | 41.8 | 47.7 | 8.7 | 1.8 | 94.22 | 23.77 | 70.45 |
| OA24-198-3 | 42.0 | 33.4 | 8.7 | 5.6 | 55.9 | 63.6 | 41.2 | 47.9 | 9.0 | 1.9 | 94.73 | 23.78 | 70.95 |
| SM1046 | 42.8 | 28.6 | 14.2 | 6.1 | 58.6 | 65.0 | 43.2 | 47.3 | 7.9 | 1.6 | 94.13 | 23.60 | 70.53 |

Total (T-AM), free (F-AM) and lipid-complexed (L-AM) amylose content, and swelling power of starch (SSP) were determined as described in the text. The percentage of A granules was calculated from the particle size distribution as particles with diameter between 10 and 35 μm. Melting temperature, $T_m$, was determined by DSC. Amylopectin chain length distribution was divided into four groups according to the DP, as described in the text. Long period $L_p$, hard block thickness $L_c$ and soft block thickness $L_a$, were calculated from SAXS curves as described in the text.

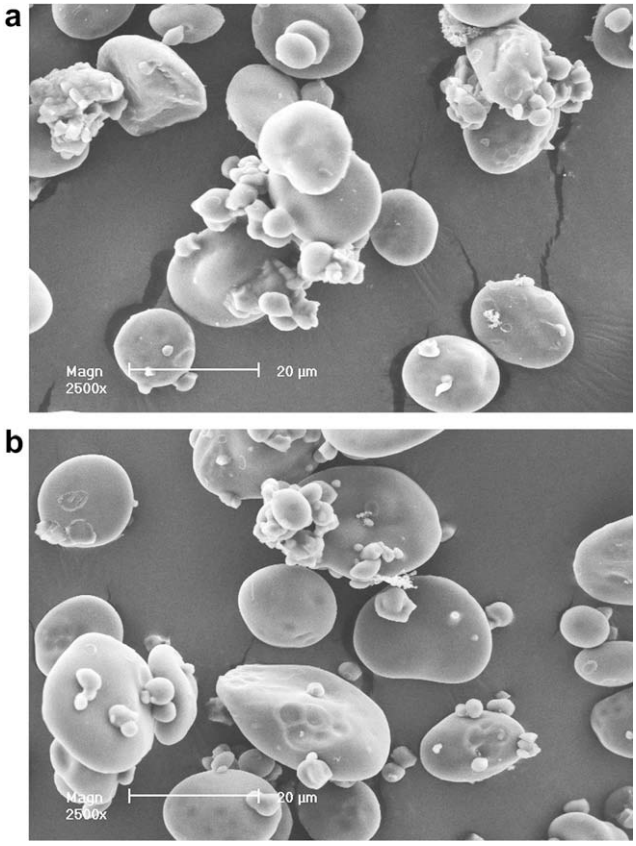


**Fig. 1.** SEM micrographs of waxy wheat starch granules (a) and SM1118 starch granules (b).

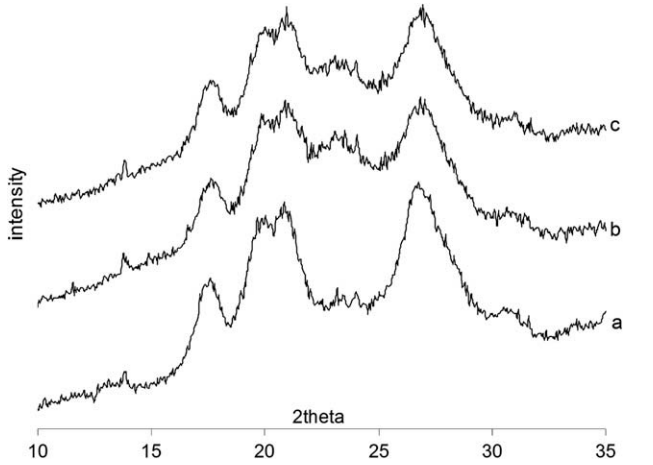


**Fig. 2.** X-ray diffraction patterns of wheat varieties used in this study. Waxy wheat (a), commercial starch (b) and SM1046 (c). The traces have been offset for clarity of presentation.

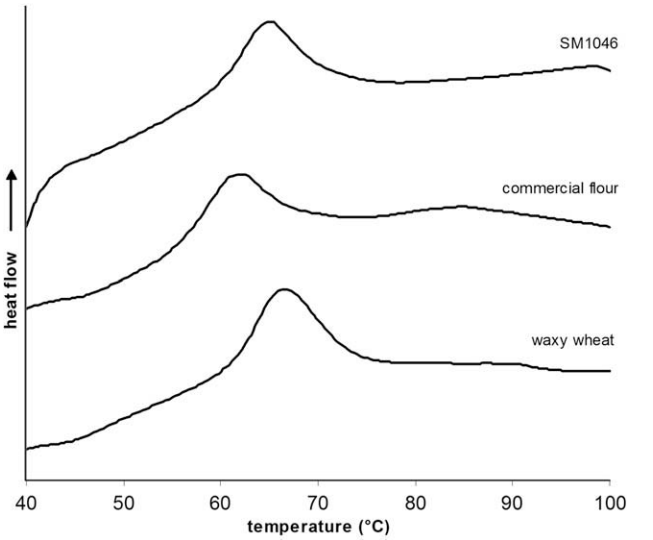


**Fig. 3.** DSC gelatinization characteristics of selected wheat varieties used in this study. Heat flow was measured in cal/sec/g and the traces have been offset for clarity of presentation. Starch to water in a ratio of 1:2, was heated at 10 °C/min.

### 3.4. SAXS characteristics

The SAXS patterns from several of the starches used in this study are shown in Fig. 4. The values of the parameters obtained from the scattering profile as described in Section 2 varied significantly among the varieties, as shown in Table 1. Long period, $L_p$, ranged between 91.8 and 94.7 Å for the starches from the VAWCRC program. The thickness of the crystalline region of the lamella (hard block), $L_c$, and amorphous region (soft block) thickness, $L_a$, varied from 68.4 to 70.9 Å and from 23.4 to 23.9 Å, respectively

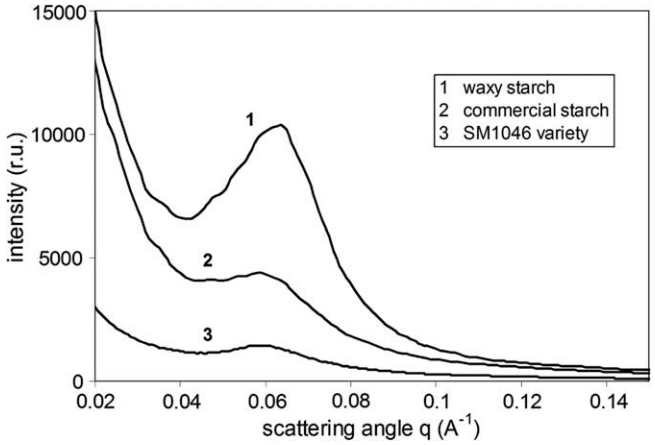


**Fig. 4.** SAXS patterns of several of the starch varieties used in this study. The traces were obtained as described in Section 2.

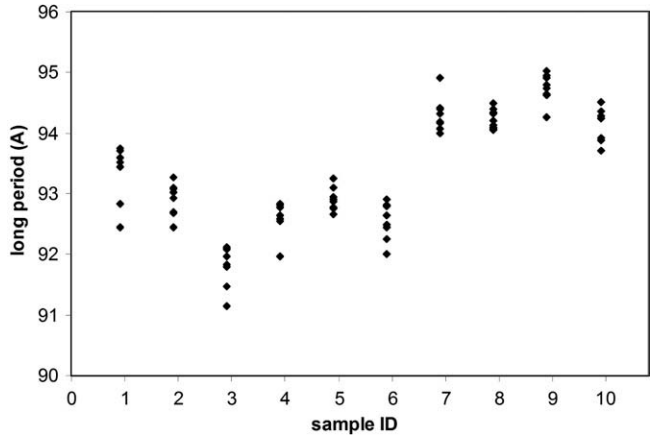


**Fig. 5.** Variability in long period based on nine replicates shown for 10 samples used in this study.

(Table 1). Fig. 5 shows nine replicate values of $L_p$ for each of the 10 samples. The variation among the replicates of each sample was within approximately 1 Å (Fig. 5). The variation in the intensity of the scattering peak within the nine replicates was comparable in magnitude to the variation among individual samples (data not shown). A similar observation was made for electron density contrast values calculated from the one dimensional correlation function. Therefore, these two parameters were not used in the statistical correlation analysis.

As determined by the graphical method of Yuryev et al. (2004), the waxy starch and commercial variety had repeat distances of 99.6 Å and 108.3 Å, respectively. As a comparison, graphical analysis performed on one of the replicate SAXS curves of variety SM1046 yielded a repeat distance of 110.2 Å. It is worth noting that the average repeat distance as determined by the correlation function analysis (Table 1) is about 15% smaller than the Bragg distance $d$, and this is in agreement with results reported by others (Jenkins, Cameron, & Donald, 1993; Yuryev et al., 2004).

Correlations of the parameters obtained from the SAXS peak with selected chemical and functional characteristics of the starch varieties used in this study (excluding the waxy wheat and commercial starch) are summarized in Table 2. Positive correlation (significant at $p < 0.05$) was found between $L_p$ and T-AM ($r = 0.75$, Fig. 6). Similarly, correlations were found between hard and soft block thicknesses and T-AM, with correlation coefficients of 0.749 and 0.669, respectively. Melting temperature and amylopectin chain length distribution did not correlate significantly with any of the studied characteristics.

## 4. Discussion

### 4.1. Repeatability of SAXS measurement

As shown by the spread of nine replicate values of $L_p$ for each of the 10 samples studied (Fig. 5), the repeatability of individual measurements was within a range of approximately 1 Å. In comparison, the variation of $L_p$ among the samples with amylose content between 36% and 43% was of the order of 3 Å. Uncertainty may exist as to whether the magnitude of the experimental error allows meaningful differentiation of such samples, given their amylose content falls within a narrow range. However, our study illustrates that SAXS may provide information regarding the lamellar architecture in sample sets that differ in $L_p$ by only a few angstroms and that a significant correlation exists between the lamellar repeat distance and amylose content.

The scattering intensity for a simple two phase system is proportional to the product of the relative fractions of each phase and the scattering length density difference (Glatter & Kratky, 1982; Higgins & Benoit 1997). In agreement with this scattering theory and according to Yuryev et al. (2004), the intensity of the scattering peak ($I_{max}$) depends on the amount of the ordered semi-crystalline structures and/or on the differences in electron density between crystalline and amorphous layers. Because the degree of crystallinity in the starches studied did not vary significantly as shown by the XRD, we propose that the observed changes in $I_{max}$ mainly reflect the difference in the electron density between the crystalline and amorphous regions of the lamellar structure. The fact that the variation in $I_{max}$ values among replicate measurements was comparable in magnitude to the variation between samples may be attributed to variations in packing density of individual capillaries influencing the scattering intensity to an extent that exceeds any correlation. As a result, natural variation between sample preparations may outweigh any real correlations. The development of a more reproducible method to avoid such variations in the packing density of these starch slurries would help overcome this issue.

### 4.2. Effect of amylose content on the structural parameters of starch granules

The results of several studies have shown that lamellar repeat distance of starches from different botanical sources varies within a range between 9 and 11 nm, and that XRD patterns show little variability within plant species (Kozlov et al., 2007a; Vandeputte & Delcour, 2004; Yuryev et al., 2004). However, starch granules extracted from different plant sources are usually considered to display decreasing intensity of the scattering maximum with increasing amylose content (Bocharnikova et al., 2003; Jenkins & Donald, 1995; Kozlov et al., 2007a; Kozlov et al., 2007b; Sanderson, Daniels, Donald, Blennow, & Engelsen, 2006; Yuryev et al., 2004). This trend is accounted for by a decrease in the difference in electron density between the crystalline and amorphous regions of the lamellae with increasing amylose content. Kozlov et al. (2007b) suggested that an increase in amylose content is accompanied both by accumulation of amylose tie-chains in amylopectin clusters forming defects in crystalline lamellae, and by disordered amylose chains within amorphous regions. Disordered ends of amylopectin double helices and/or double helices not participating in the formation of crystals are also proposed to be contributing factors to defects of the crystalline regions and, in turn, to greater disorder in the packing of the lamellar structure (Koroteeva et al., 2007a; Koroteeva et al., 2007b; Kozlov et al.,

**Table 2**
Correlation matrix between physicochemical and structural characteristics, based on the 10 samples used in this study

| | T-AM | F-AM | L-AM | SSP | A granules | $T_m$ | DP 6–12 | DP 13–24 | DP 25–36 | DP>36 |
|---|---|---|---|---|---|---|---|---|---|---|
| $L_p$ | **0.752** | 0.299 | 0.483 | −0.481 | 0.482 | −0.135 | 0.239 | −0.538 | 0.336 | 0.049 |
| $L_a$ | **0.669** | 0.421 | 0.330 | −0.467 | 0.512 | −0.016 | −0.017 | −0.254 | 0.391 | 0.148 |
| $L_c$ | **0.749** | 0.267 | 0.501 | −0.472 | 0.463 | −0.156 | 0.285 | −0.581 | 0.316 | 0.028 |
| $T_m$ | 0.368 | −0.044 | 0.360 | 0.113 | −0.070 | 1 | −0.291 | 0.475 | −0.189 | 0.141 |

Values in bold indicate significant correlations at a significance level alpha = 0.05, minimum $r$ to be significant at $p = 0.05$ for $n = 10$ samples is 0.632. Total (T-AM), free (F-AM) and lipid-complexed (L-AM) amylose content, and swelling power of starch (SSP) were determined as described in the text. The percentage of A granules was calculated from the particle size distribution as particles with diameter between 10 and 35 μm. Melting temperature, $T_m$, was determined by DSC. Amylopectin chain length distribution was divided into four groups according to the DP, as described in the text. Long period $L_p$, hard block thickness $L_c$ and soft block thickness $L_a$, were calculated from SAXS curves as described in the text.

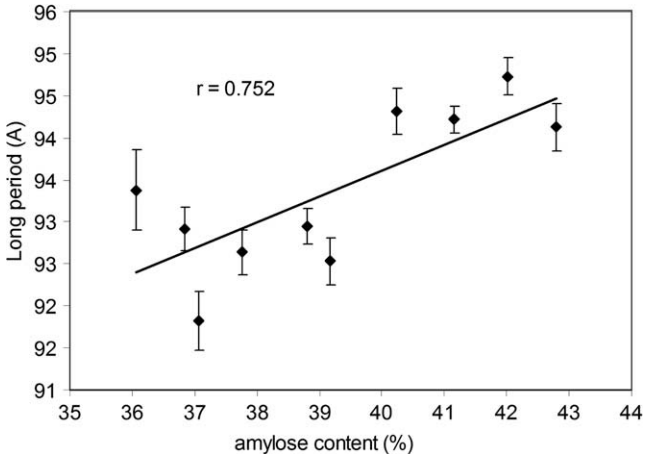


**Fig. 6.** Amylose content vs. long period. Error bars show standard deviations based on nine replicates.

2007b). The occurrence of amylose–amylose double helices within the crystalline lamellar regions containing mainly amylopectin double helices has been shown to be highly unlikely in native starch granules and is not considered as a possible explanation for the intensity decrease (Kalichevsky & Ring, 1987; Tester, Debon, & Sommerville, 2000).

Positive correlations between $L_p$ and amylose content, and between hard and soft block thicknesses and amylose content, indicate that amylose accumulates in both crystalline and amorphous parts of the lamellae (Table 2 and Fig. 6). This hypothesis is consistent with current understanding of starch synthesis, which considers that amylose and amylopectin are synthesized simultaneously (reviewed by Morell, Regina, Li, Hashemi, & Rahman, 2003). If thickness of one of the lamellar regions remained constant as the amylose content varies, it would be more difficult to explain how amylose and amylopectin are synthesized together and packed into the granule.

It has been reported that an increase in amylose content would be expected to be accompanied by decreasing crystallinity, decreasing melting enthalpy and decreasing values of melting temperature of the amylopectin crystallites in native wheat starch granules with amylose content less than 50% (Koroteeva et al., 2007a; Koroteeva et al., 2007b; Kozlov et al., 2007b). In agreement with results by Hung et al. (2008), our results did not confirm these trends. Insignificant differences in total crystallinity and the lack of correlation between $T_m$ and any of the studied characteristics within the set of varieties from VAWCRC program indicates that there may be several underlying factors affecting lamellar structure that may mask general trends that occur over a wider range of amylose content. Increased defects in the crystalline lamella with increasing amylose content may to some extent be compensated by a protective effect of amylose in the amorphous lamellar regions on the crystallites, consistent with increased soft block thickness being correlated with increasing amylose content.

The SAXS curves shown in Fig. 4 indicate that the contrast in electron density between hard and soft blocks of waxy starch is significantly greater than in the other starches, even when underlying variability in scattering peak intensity is considered. When the waxy wheat variety was compared with the other varieties used in this study, the following trends were observed: the waxy variety had more sharply defined XRD peaks, smaller repeat distance, higher intensity of the SAXS peak, higher melting temperature, and higher melting enthalpy. Based on combined results acquired by SAXS, DSC and XRD analyses, we conclude that the differences between the waxy variety and the other samples used in this study are due to amylose defects accumulating in the crystalline regions as well as more amylose accumulating in the amorphous regions of lamellar structure. The higher melting temperature, more sharply defined XRD peaks and greater intensity of SAXS peak observed for the waxy starch are consistent with the hypothesis that amylopectin crystallites have fewer defects in waxy starch than in amylose-rich starches. The larger lamellar repeat distance observed for the non-waxy starches provides evidence for more amylose accumulating in both crystalline and amorphous regions of the lamellae in amylose-rich starches.

Starch extracted from commercial flour had amylose content between that of waxy wheat and the set of wheat varieties from VAWCRC. Accordingly, intensity of the scattering peak and repeat distance of the commercial starch was between that of waxy wheat and the VAWCRC varieties. However, perfection of XRD peaks, melting temperature and transition enthalpy were lower than in starches from the VAWCRC varieties. We propose that crystallinity and thermal characteristics, but not electron density contrast and lamellar thicknesses, of the commercial starch may have been affected by commercial milling, for example by inclusion of a grain tempering step.

Lamellar spacing, as indicated by $L_p$, did not increase continuously with increasing amylose content, but rather the 10 samples segregated into two groups, with a step increase in $L_p$ between them (Fig. 6). The two groups were not differentiated by growing season, and hence this distribution is likely to reflect underlying genetic variation and/or environmental influences on the expression and activities of enzymes involved in starch synthesis.

Over a wide range of amylose content, three main factors are considered to influence the structural parameters of native starch granules at the nanoscale: (i) amylose defects located in the crystalline region of the lamellae (both as amylose tie-chains and amylose–lipid complexes), (ii) the amount of amylose within the amorphous regions of the lamellae, and (iii) chain length distribution of amylopectin chains (Koroteeva et al., 2007a; Koroteeva et al., 2007b; Kozlov et al., 2007b). When structural characteristics of the group of amylose-rich starches used in this study were compared with waxy wheat starch, the general trend described by Kozlov et al. (2007b) was confirmed. However, our results indicate that

increasing amylose content within a narrow range of elevated amylose content is not necessarily accompanied by increased accumulation of crystal defects. In general, the structure of wheat starches from different varieties, and their functional properties, appear to be determined by amylose content, but fine structural variations brought about by differences in genetic background introduces uncertainty into the prediction of functional properties from amylose content alone.

## 5. Conclusions

Analysis of starches with amylose content between 36% and 43% showed SAXS may provide information regarding the lamellar architecture in sample sets that differ in $L_p$ by only a few angstroms and that a significant correlation exists between the lamellar repeat and amylose content. The results of the SAXS analysis of the wheat starches were consistent with amylose accumulating in both crystalline and amorphous parts of the lamellae. We conclude that amylose content directly affects the organization of semi-crystalline lamellae within granules, whereas thermodynamic properties are influenced more by the interplay between amylose content and amylopectin architecture.

## Acknowledgements

J.B. was supported by a scholarship from the Value Added Wheat CRC Ltd. The authors acknowledge the facilities as well as scientific and technical assistance from staff in the NANO Major National Research Facility at the Electron Microscope Unit, The University of Sydney. The authors are grateful to Allied Mills for use of the laboratory mill Quadramat Junior and Mastersizer particle size instrument. The authors are also grateful to CSIRO Plant Industries, Canberra for making available the Beckman P/ACE System 5010 Capillary Electrophoresis Instrument and to Oscar Larroque for assistance with the analysis.

## References

Akerberg, A. K. E., Liljeberg, H. G. M., Granfeldt, Y. E., Drews, A. W., & Bjorck, I. M. E. (1998). An in vitro method, based on chewing, to predict resistant starch content in foods allows parallel determination of potentially available starch and dietary fiber. *Journal of Nutrition, 128*, 651–660.

Balta Calleja, F. J., & Vonk, C. G. (1989). *X-ray Scattering of Synthetic Polymers*. Amsterdam: Elsevier. pp. 247–257.

Blanshard, J. M. V., Bates, D. R., Muhr, A. H., Worcester, D. L., & Higgins, J. S. (1984). Small angle neutron scattering studies of starch granule structure. *Carbohydrate Polymers, 4*, 427–442.

Blazek, J., & Copeland, L. (2008). Pasting and swelling properties of wheat flour and starch in relation to amylose content. *Carbohydrate Polymers, 71*, 380–387.

Bocharnikova, I., Wasserman, L. A., Krivandin, A. V., Fornal, J., Baszczak, W., Chernykh, V. K., et al. (2003). Structure and thermodynamic melting parameters of wheat starches with different amylose content. *Journal of Thermal Analysis and Calorimetry, 74*, 681–695.

Cameron, R. E., & Donald, A. M. (1992). A small-angle X-ray scattering of study of the annealing and gelatinisation of starch. *Polymer, 33*, 2628–2635.

Chrastil, J. (1987). Improved colourimetric determination of amylose in starches of flours. *Carbohydrate Research, 159*, 154–158.

Daniels, D. R., & Donald, A. M. (2003). An improved model for analyzing the small-angle x-ray scattering of starch granules. *Biopolymers, 69*, 165–175.

Donald, A. M., Kato, K. L., Perry, P. A., & Waigh, T. A. (2001). Scattering studies of the internal structure of starch granules. *Starch/Stärke, 53*, 504–512.

Glatter, O., & Kratky, O. (1982). *Small-angle X-ray Scattering*. New york: Academic Press.

Higgins, J. S., & Benoit, H. C. (1997). *Polymers and Neutron Scattering*. Oxford University Press. pp. 124.

Hung, P. V., Maeda, T., Miskelly, D., Tsumori, R., & Morita, N. (2008). Physicochemical characteristics and fine structure of high-amylose wheat starches isolated from Australian wheat cultivars. *Carbohydrate Polymers, 71*, 656–663.

Hung, P. V., Maeda, T., & Morita, N. (2007). Study on physicochemical characteristics of waxy and high-amylose wheat starches in comparison with normal wheat starch. *Starch/Stärke, 59*, 125–131.

Jenkins, P. J., Cameron, R. E., & Donald, A. M. (1993). A universal feature in the structure of starch granules from different botanical sources. *Starch/Stärke, 45*, 417–420.

Jenkins, P. J., & Donald, A. M. (1995). The influence of amylose on starch granule structure. *International Journal of Biological Macromolecules, 17*, 315–321.

Kalichevsky, M. T., & Ring, S. G. (1987). Incompatibility of amylose and amylopectin in aqueous solution. *Carbohydrate Research, 162*, 323–328.

Koberstein, J. T., & Stein, R. J. (1983). Small-angle x-ray scattering measurements of diffuse phase-boundary thicknesses in segmented polyurethane elastomers. *Journal of Polymer Science: Polymer Physics Edition, 21*, 2181–2200.

Koroteeva, D. A., Kiseleva, V. I., Krivandin, A. V., Shatalova, O. V., Błaszczak, W., Bertoft, E., et al. (2007a). Structural and thermodynamic properties of rice starches with different genetic background. Part 2. Defectiveness of different supramolecular structures in starch granules.. *International Journal of Biological Macromolecules, 41*, 534–547.

Koroteeva, D. A., Kiseleva, V. I., Sriroth, K., Piyachomkwan, K., Bertoft, E., Yuryev, P. V., et al. (2007b). Structural and thermodynamic properties of rice starches with different genetic background. Part 1. Differentiation of amylopectin and amylose defects. *International Journal of Biological Macromolecules, 41*, 391–403.

Konik-Rose, C. M., Moss, R., Rahman, S., Appels, R., Stoddard, F., & McMaster, G. (2001). Evaluation of the 40 mg swelling test for measuring starch functionality. *Starch/Stärke, 53*, 14–20.

Kozlov, S. S., Blennow, A., Krivandin, A. V., & Yuryev, V. P. (2007a). Structural and thermodynamic properties of starches extracted from GBSS and GWD suppressed potato lines. *International Journal of Biological Macromolecules, 40*, 449–460.

Kozlov, S. S., Krivandin, A. V., Shatalova, O. V., Noda, T., Bertoft, E., Fornal, J., et al. (2007b). Structure of starches exctracted from near-isogenic wheat lines. Part II. Molecular organization of amylopectin clusters.. *Journal of Thermal Analysis and Calorimetry, 87*, 575–584.

Kozlov, S. S., Noda, T., Bertoft, E., & Yuryev, V. P. (2006). Structure of starches exctracted from near-isogenic wheat lines. Part I. Effect of different GBSS I combinations. *Journal of Thermal Analysis and Calorimetry, 86*, 291–301.

Lopez-Rubio, A., Htoon, A., & Gilbert, E. P. (2007). Influence of extrusion and digestion on the nanostructure of high-amylose maize starch. *Biomacromolecules, 8*, 1564–1572.

Lopez-Rubio, A., Flanagan, B. M., Gilbert, E. P., & Gidley, M. J. (2008). A novel approach for calculating starch crystallinity and its correlation with double helix content: a combined XRD and NMR study. *Biopolymers, 89*, 761–768.

Matveev, Y. I., Elankin, N. I., Kalistratova, E. N., Danilenko, A. N., Niemann, C., & Yuryev, V. P. (1998). Estimation of contributions of hydration and glass transition to heat capacity changes during melting of native starches at excess water. *Starch/Stärke, 50*, 141–147.

Morell, M. K., Samuel, M. S., & O'Shea, M. G. (1998). Analysis of starch structure using fluorophore-assisted carbohydrate electrophoresis. *Electrophoresis, 19*, 2603–2611.

Morell, M. K., Regina, A., Li, Z., Hashemi, B. K., & Rahman, S. (2003). Advances in the understanding of starch synthesis in wheat and barley. *Journal of Applied Glycoscience, 50*, 217–224.

Morell, M. K., & Myers, A. M. (2005). Towards the rational design of cereal starches. *Current Opinion in Plant Biolology, 8*, 204–210.

O'Shea, M. G., Samuel, M. S., Konik, C. M., & Morell, M. K. (1998). Fluorophore-assisted carbohydrate electrophoresis (FACE) of oligosaccharides: efficiency of labelling and high-resolution separation. *Cabohydrate Research, 307*, 1–12.

Sanderson, J. S., Daniels, R. D., Donald, A. M., Blennow, A., & Engelsen, S. B. (2006). Exploratory SAXS and HPAEC-PAD studies of starches from diverse plant genotypes. *Carbohydrate Polymers, 64*, 433–443.

Strobl, G. R., & Schneider, M. (1980). Direct evaluation of the electron density correlation function of partially crystalline polymers. *Journal of Polymer Science: Polymer Physics Edition, 18*, 1343–1359.

Tester, R. F., Debon, S. J. J., & Sommerville, M. D. (2000). Annealing of maize starch. *Carbohydrate Polymers, 42*, 287–299.

Vandeputte, G. E., & Delcour, J. A. (2004). From sucrose to starch granule to starch physical behaviour: a focus on rice starch. *Carbohydrate Polymers, 58*, 245–266.

Vermeylen, R., Derycke, V., Delcour, J. A., Goderis, B., Reynaers, H., & Koch, M. H. J. (2006). Gelatinization of starch in excess water: beyond the melting of lamellar crystallites. a combined wide- and small-angle X-ray scattering study. *Biomacromolecules, 7*, 2624–2630.

Vermeylen, R., Goderis, B., Reynaers, H., & Delcour, J. A. (2005). Gelatinisation related structural aspects of small and large wheat starch granules. *Carbohydrate Polymers, 62*, 170–181.

Waigh, T. A., Gidley, M. J., Komanshek, B. U., & Donald, A. M. (2000a). The phase transformations in starch during gelatinisation: a liquid crystalline approach. *Carbohydrate Research, 328*, 165–176.

Waigh, T. A., Jenkins, P. J., & Donald, A. M. (1996). Quantification of water in carbohydrate lamellae using SANS. *Farraday Discussions, 103*, 325–337.

Waigh, T. A., Kato, K. L., Donald, A. M., Gidley, M. J., & Riekel, C. (2000b). Side-chain liquid crystalline model for starch. *Starch/Stärke, 52*, 252–260.

Waigh, T. A., Perry, P., Riekel, C., Gidley, M., & Donald, A. M. (1998). Chiral side-chain liquid-crystalline properties of starch. *Macromolecules, 31*, 7980–7984.

Yuryev, V. P., Krivandin, A. V., Kiseleva, V. I., Wasserman, L. A., Genkina, N. K., Fornal, J., et al. (2004). Structural parameters of amylopectin clusters and semi-crystalline growth rings in wheat starches with different amylose content. *Carbohydrate Research, 339*, 2683–2691.